

Simulation of Class D resonance inverter for Acoustics Energy Transfer applications

Huzaimah Husin

Faculty of Electronics & Computer Engineering
Universiti Teknikal Malaysia Melaka
Melaka, Malaysia
huzaimah@utem.edu.my

H. Hamidon

Faculty of Electronics & Computer Engineering
Universiti Teknikal Malaysia Melaka
Melaka, Malaysia
hamid@utem.edu.my

Shakir Saat

Faculty of Electronics & Computer Engineering
Universiti Teknikal Malaysia Melaka
Melaka, Malaysia
shakir@utem.edu.my

Y. Yusmarnita

Faculty of Electronics & Computer Engineering
Universiti Teknikal Malaysia Melaka
Melaka, Malaysia
yusmarnita@utem.edu.my

Abstract – Power conditioning stage of an acoustics energy transfer (AET) is a key step in determining the overall efficiency of the AET system. On the transmitter side, it needs to drive the device at the exact operating frequency meanwhile at the receiver side, it need to able to extract maximum power through interfacing with PZT transducer. This paper will study and simulate the Class D parallel-resonance inverter for the transmitter side of an AET system. The aimed of the circuit is to produce around 80 mW power at the operating frequency 416 kHz for implantable applications. The Proteus Software used as simulation platform with peripheral interface controller (PIC16F877A) as pulse width modulation signal generator. The pulse width modulation (PWM) used to generate switching signal for MOSFET IRF5852TR gate in the circuit.

Keywords—*Half-bridge Class D inverter; low power applications*

I. INTRODUCTION

In certain application areas, contactless energy transfer or wireless power transfer (WPT) is increasingly being considered to be viable alternative for the power supply of electronics. Consumer products employ WPT to charge batteries of mobile devices without having to use an adaptor [1]. It also used in industry in linear and planar actuators in which the wear of cable slabs and the parasitic force that exerted have to be minimized [2]. Lastly, WPT can also be applied to charge microbatteries in biomedical implants [3]. The contactless transmission of energy consists a number of established technologies such as inductive energy transfer (IET), capacitive energy transfer (CET), far-field electromagnetic coupling (EM) and optical coupling. A relatively new method is acoustic energy transfer (AET) that uses vibration or ultrasound waves to propagate energy without relying on electrical contact. AET is an effective method for powering implanted devices such as pacemakers, defibrillators, heart-assist devices and implanted insulin pumps. Some of the implanted devices are designed to serve monitoring purposes such as biosensors, glucose indicators. Even though IET has been receiving considerable attention lately, with the recent publications on systems delivering energy over distances up to 2 m at high efficiencies [4] and [5] but due to the magnetic coupling technique, IET

is not suitable for transferring the power across metal objects and can cause large eddy current losses [6],[7] and [8]. In order to overcome these limitations, CET is used since an electric field can penetrate through any metal shielding environment. The CET not only can transmit through metal and shielded body, but also has good anti-interference ability of magnetic field [7],[8],[9] and [10]. However, till recent, CET systems have only been used for very low power delivery applications [6], [8],[9] and [10]. CET is used far less often due to the limitation of distance that can be crossed with it. This is a direct consequence of the inverse proportionality of the capacitance with the distance, requiring high voltages and frequencies for the transfer of a certain amount of power.

Another principle for WPT is far-field EM or microwave energy transfer is seldom used. Instead of the nonradiative used in inductive and capacitive cases, a radiative EM field functions as the energy transfer medium. Rectification of these high-frequency waves at the pick-up unit can be achieved at high efficiency of 80% - 90% [11]. Generation of the microwaves, on the other hand, is much more difficult, particularly when a solid-state RF generator is used.

Optical energy transmission uses same principle as far-field EM and has low efficiency whereby 40% and 50% of energy is lost [10] and [12].

All the previously described methods rely on EM fields for the transfer of power. The radiative wave that is used in microwave and optical WPTs hints at an entirely different way of wireless conveying power. One just has to realize that such a wave does not have to be of an EM nature but that any type of wave can be used for this purpose. The choice of using sound wave or ultrasonic waves therefore seems a reasonable one.

II. ACOUSTICS ENERGY TRANSFER CONCEPT

Impracticality the use of battery and physically wired for the implantable devices inspires this research to be carried out. The application of ultrasound or vibration as the medium of energy transmission especially in situations where no EM fields are allowed, and high directionality of the power transfer in combination with small system dimensions is required [10] and [12].

A. AET System

The basic structure of AET system is shown in Fig. 1. This system consists of transmitter unit and receiver unit. On the transmitter unit, external transducer usually PZT transducer will be attached to the skin surface and facing an implanted transducer at the receiver unit.

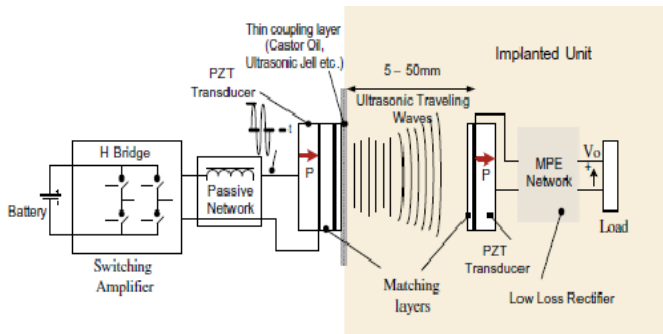


Fig. 1. Acoustic Energy Transfer system [3]

An electrical power source, a DC will energizes the transmitter transducer that converts the electrical energy to vibration or acoustics pressure waves. The acoustic waves will propagates and carry the energy through the tissue toward an implanted receiver transducer that positioned within the radiation lobe of the transmitter. A receiving unit functions for the inverse process of converting the vibration or motion caused by the waves into electrical energy. A rectifier will rectify that particular electrical energy and filters the output voltage of the receiving transducer. The usable steady dc voltage drives a load. In order to minimize the inconvenience caused to the patient as well as to ensure a close fit to the body (which is required for good acoustic coupling), the

device should be light in weight and thin so that its center of gravity is as close as possible to the surface of the skin.

B. Power Conditioning

The overall efficiency of AET system will be determined by the power conditioning stage in the circuit. It is requires to drive the device at the exact operating frequency without exciting harmonic modes at the transmitter unit. On the receiver unit, the circuit should interface with the transducer so as to extract maximum power. The power conditioning circuit on the both sides must have efficiency >80% as they affect the overall efficiency of the energy transfer. This paper will focus on powering the transmitter unit of AET system. The CLASS D inverter is one of the high-frequency high-efficiency resonant power sources, which has been applied to dc/dc resonant converters, radio transmitters, and electronic ballasts for fluorescent lamps[13] and [14]. Its high dc/ac power conversion efficiency is achieved by the zero-current switching (ZCS), which enables its operation at frequency of several hundred kilohertz. Furthermore, this resonant inverter with sinusoidal waveforms achieves low switching losses due to the phase displacement between the voltage and current through the transistors [15].

C. Power Requirement

The key to settling the impracticality the use of battery and physically wired for the implantable devices problem is by having the continuous supply of a stable power source. In most cases, the devices has to be replaced just because of the battery is running out inside the device. Therefore, it is the battery that determines the longevity of the devices. Although the requirement of each device is different, the power that needed generally falls in the level of μW – mW as in Table 1.

TABLE 1. POWER REQUIREMENT FOR IMPLANTABLE DEVICES [16]

Implanted devices	Typical power requirement
Pacemaker	30 μ -100 μ W
Cardiac defibrillator	30 μ -100 μ W
Neurological simulator	30 μ to several mW
Drug pump	100 μ to 2mW
Cochlear implant	10mW

III. THEORETICAL RESULTS

In order to design the transmitter side, which focuses on half-bridge Class D parallel-resonance inverter, the theoretical value of each components is obtained through calculation. The equations related were explained in details in [17]. The calculation based on the standard circuit shown in Fig. 2.

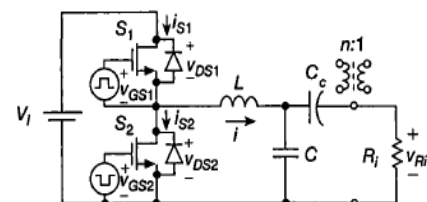


Fig. 2. Standard Circuit of the Class D parallel resonant inverter [17]

A. Principle of operation

A standard circuit of half-bridge Class D voltage-source parallel-resonant inverter (PRI) is shown in Fig.2. It consists of two switches S_1 and S_2 , a resonant inductor L , a resonant capacitor C , and a DC-blocking capacitor C_c . Resistance R_i represents a load to which the AC power is to be delivered and is connected in parallel with the resonant capacitor C . The average voltage across capacitor C_c is equal to $V_1/2$. The two bidirectional switches S_1 and S_2 and the DC input voltage source V_1 form a square-wave voltage source that drives the resonant circuit L - C - R_i . Switches S_1 and S_2 are alternately turned ON and OFF at the switching frequency $f = \omega/2\pi$. Because of the turn-off delay time of power MOSFETs, the duty cycle of drive voltages V_{GS1} and V_{GS2} should be slightly less than 50% to avoid cross conduction.

B. Assumptions of analysis

The analysis of the inverter in Fig. 2 assumes

- i. Each switch is a resistance r_{DS} when “on” and an open circuit when “off”.
- ii. Switching losses are neglected.
- iii. The loaded quality factor Q_L of the resonant circuit is high enough so that the currents through inductance L , capacitance C , and resistance R_i is sinusoidal.
- iv. The coupling capacitance C_c is high enough so that its AC voltage ripple is negligible.
- v. The output capacitances of MOSFETs are neglected.

C. Design parameters

- i. Input voltage, $V_1 = 3.6\text{Vdc}$
- ii. Output power, $P_{Ri} = 80\text{ mW}$
- iii. Resonant frequency, $f_r = 416\text{ kHz}$.
- iv. Quality factor, $Q_L = 2.5$

D. Equations

In order to get theoretical value of components, some equations used as stated as below.

Assume a typical value of the inverter efficiency $\eta_I = 95\%$, some relevant equations as below:

DC supply power is

$$P_1 = \frac{P_{Ri}}{\eta_I} \text{ W} \tag{1}$$

DC supply current is

$$I_1 = \frac{P_1}{V_1} \text{ A} \tag{2}$$

Assuming $f = f_r = 416\text{ kHz}$ at full power, the corner frequency is

$$f_o = \frac{f_r}{\sqrt{1 - \frac{1}{Q_L}}} \text{ Hz} \tag{3}$$

The AC load resistance

$$R_i = \frac{V_{Ri}^2}{P_{Ri}} = \frac{2V_1^2 \eta_I^2}{\pi^2 P_{Ri} \left(\left[1 - \left(\frac{\omega}{\omega_o} \right)^2 \right]^2 + \left[\frac{1}{Q_L} \left(\frac{\omega}{\omega_o} \right) \right]^2 \right)} \Omega \tag{4}$$

The characteristic impedance can be obtained as

$$Z_o = \frac{R_i}{Q_L} \Omega \tag{5}$$

Thus, the elements of resonant circuits are

$$L = \frac{Z_o}{\omega_o} \text{ Henry} \tag{6}$$

and

$$C = \frac{1}{\omega_o Z_o} \text{ Farad} \tag{7}$$

The maximum value of the switch peak current is

$$I_{m(max)} = I_{SM(max)} = \frac{2V_1 \sqrt{Q^2 L + 1}}{\pi Z_o} \text{ A} \tag{8}$$

The voltage stresses on the resonant components are

$$V_{Cm(max)} = \frac{2V_1 Q_L}{\pi} \text{ V}, \quad V_{Lm(max)} = \frac{2V_1 \sqrt{Q^2 L + 1}}{\pi} \text{ V} \tag{9}$$

As the load is in parallel with resonant capacitor as shown in Fig. 2, the output voltage at the load can be obtained as

$$V_o = V_{cm} V \quad (10)$$

As the aim of this paper is to produce output power at R_i , the equation below use to calculate the output power required.

$$P_{Ri} = \frac{V_{orms}^2}{R_i} \quad (11)$$

The selection of IRF5852TR as a switching MOSFET due to suitable voltage rating and power dissipation regards to design specifications.

Using equations (1)-(11), the theoretical value of each component and parameter were calculated and tabulated in Table 2.

TABLE 2. CALCULATION VALUE FOR EACH COMPONENT AND PARAMETERS FOR INVERTER

Inverter Parameters	Symbol	Value
Dc Supply Power	P_1	84.21 mW
Dc Supply Current	I_1	23.4 mA
Corner frequency	f_o	453.89 kHz
AC Load Resistance	R_i	185.28 Ω
Impedance	Z_o	74.11 Ω
Resonant Inductor	L	25.9 μ H
Resonant Capacitor	C	4.73 nF
Switch Peak Current	$I_{m(max)}$	83.2 mA
Voltage at resonant Capacitor	$V_{Cm(max)}$	5.73 V
Voltage at resonant Inductor	$V_{Lm(max)}$	6.17 V
Output power gained	P_{Ri}	88.6 mW

IV. SIMULATION RESULTS

In order to verify the designed model, simulation through Proteus Software where the inputs signal PWM was generated by peripheral interface controller (PIC16F877A). The coding for the PWM was built using mikroC PRO for PIC software.

A. The design of power amplifier Circuit

The circuit designed by applying MOSFET IRF5852TR as a switch that turns on and off alternately at the switching frequency, $f = \frac{\omega}{2\pi}$. The square wave signal as a driver for those MOSFETs was generated by PIC and

feed in to the gate of the MOSFET. The designed circuit is shown in Fig. 3.

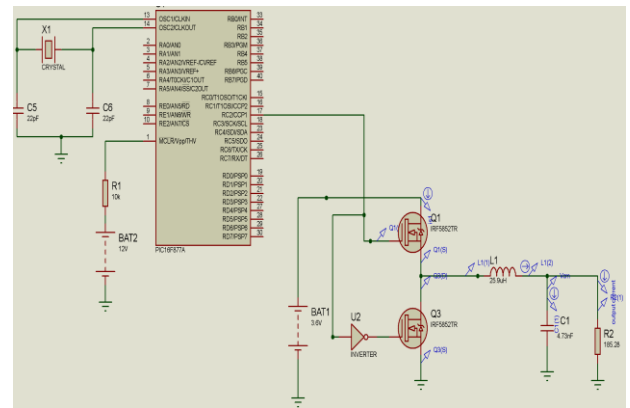


Fig. 3. The schematic of Class D Parallel-resonant inverter simulation

Proteus simulation has been undertaken to analyze the functionality of the designed circuit. The components value selection was based on the previous calculation as tabulated in Table 2.

B. The Gate Signal for MOSFET

The generation of PWM was done by PIC16F877A with the coding simulation through mikroC PRO for PIC software. The generation of 5Vp square wave is produced by PIC with the resonant frequency 416 kHz is successfully obtained and shown in Fig. 4. A 5Vp square wave input that drives the resonant circuit $L-C-R_i$ is connected to the gate of S_1 meanwhile the inverted is connected to the gate of S_2 . The inversion is done in order to fulfill the out-of-phase condition between S_1 and S_2 and shown in Fig. 5.

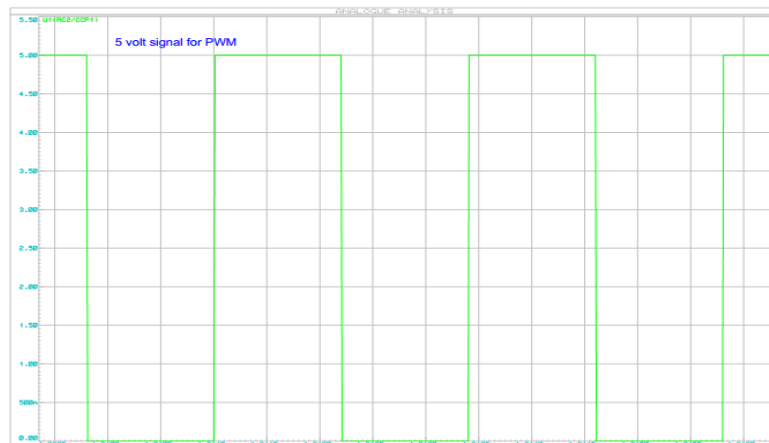


Fig. 4. Simulated gate signal generated by PIC

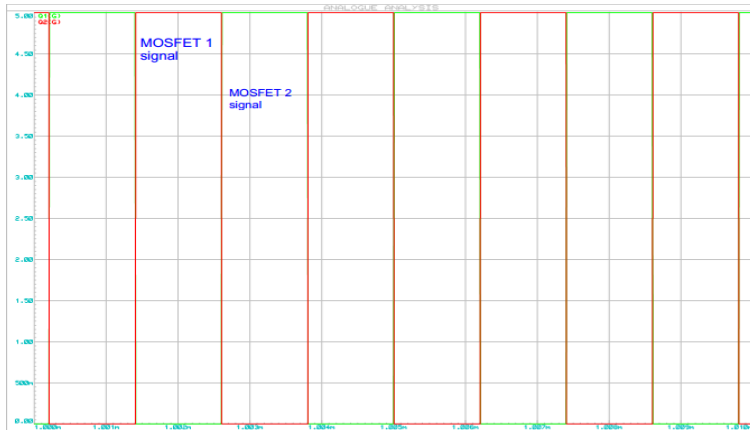


Fig. 5. Simulated gate signal for MOSFET

C. The Output Power of the circuit

This paper concentrated on producing low power output for implantable devices that uses acoustic as medium of propagation. The output power calculated by using equation (10) and (11). Fig. 6 shows the simulated output voltage of the inverter.

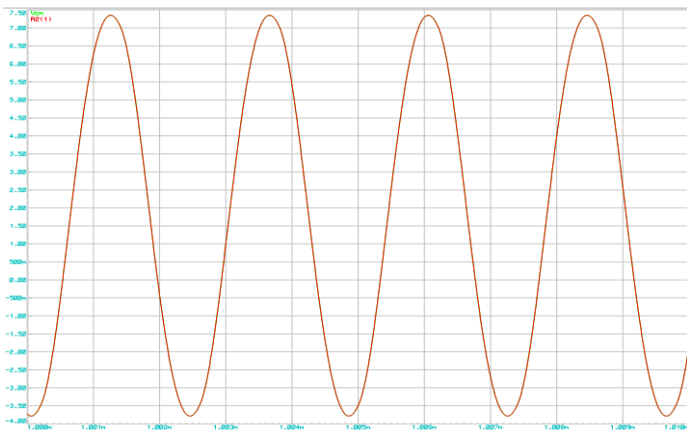


Fig.6 . Simulated output voltage of the inverter

From the graph, the peak-peak output voltage is 11.2 V; meanwhile the peak output voltage is 5.6 V. The fully sinusoidal waveform is successfully obtained at the output voltage thus consistent with the purpose of inverter that converted a DC voltage to an AC voltage. The output power was measured at the point of AC load resistor, R_i . The waveform similarity also can be founded between V_{Cm} and V_o due to their parallel arrangement. From calculation, $V_o = V_{Cm} = 5.73$ V, meanwhile through simulation, $V_o = V_{Cm} = 5.6$ V. There is slightly different since the simulation might take into account some parasitic resistance of the components that affected the power. Using equation (11), this design obtained 84.63 mW as output power compared to 88.6 mW as in the calculation.

V. CONCLUSION

In this paper, the requirement of powering AET system at the transmitter side is studied and the circuit of power amplifier is designed. Various important components value were calculated and tabulated based on established equations. To validate the theoretical results, the simulation was undertaken and the results shows that the output voltage consistent with the Class D parallel-resonant inverter characteristics. Observed waveforms and values in the circuit simulations showed good agreement with the calculated ones. Future work on this design to consider various parameters such as load, quality factor and MOSFET selection will be done.

ACKNOWLEDGMENT

The author would like to express the appreciation to Universiti Teknikal Malaysia Melaka (UTeM) and Ministry Of Education Malaysia for funding this research work under RAGS/1/2014/TK03/FKEKK/B00062 grant.

REFERENCES

- [1] C. L. W. Sonntag, J. L. Duarte, and a. J. M. Pemen, "Load position detection and validation on variable-phase contactless energy transfer desktops," in *2009 IEEE Energy Conversion Congress Expo*, San Jose, California, 2009, pp. 1818–1825.
- [2] S. Hussmann and P. a. Hu, "A microcomputer controlled ICPT power pick-up and its EMC considerations for moving sensor applications," in *Proceedings of International Conference on Power System Technology.*, vol. 2, Kunming, China, 2002, pp. 1011–1015.
- [3] S. Ozeri and D. Shmilovitz, "Ultrasonic transcutaneous energy transfer for powering implanted devices.," in *Ultrasonics*, May 2010, vol. 50, no. 6, pp. 556–66.
- [4] A. Karalis, J. D. Joannopoulos, and M. Soljačić, "Efficient wireless non-radiative mid-range energy transfer," in *Ann. Phys. (N. Y.)*, 2008, vol. 323, pp. 34–48.
- [5] A. Kurs, A. Karalis, R. Moffatt, J. D. Joannopoulos, P. Fisher, and M. Soljagic, "Wireless power transfer via strongly coupled magnetic resonances.," in *Science*, 2007, vol. 317, no. July, pp. 83–86.
- [6] M. P. Theodoridis, "Effective capacitive power transfer," *IEEE Transaction on Power Electronics*, 2012, vol. 27, no. 12, pp. 4906–4913.
- [7] C. Liu, A. P. Hu, and M. Budhia, "A generalized coupling model for Capacitive Power Transfer systems," in *Annual*

- Conference of the IEEE Industrial Electronics Society*, Glendale, AZ, U.S.A., 2010, vol. 27, no. 12, pp. 274–279.
- [8] C. Y. Xia, C. W. Li, and J. Zhang, “Analysis of power transfer characteristic of capacitive power transfer system and inductively coupled power transfer system,” in *Proceeding . 2011 International Conference on Mechatronic Science. Electric Engineering and Computer*, Jilin, China, 2011, pp. 1281–1285.
- [9] M. Kline, I. Izyumin, B. Boser, and S. Sanders, “Capacitive power transfer for contactless charging,” in *IEEE Applied Power Electronics Conference Expo*, Forth Worth, Tx, 2011, pp. 1398–1404.
- [10] T. Zaid, S. Saat, Y. Yusop, and N. Jamal, “Contactless energy transfer using acoustic approach - A review,” in *IEEE 2014 International Conference on Computer, Communication and Control Technology*, Langkawi, Malaysia, 2014, pp. 376–381.
- [11] J. O. McSpadden and J. C. Mankins, “Space solar power programs and microwave wireless power transmission technology,” in *IEEE Microwave Magazine*, December, 2002, vol. 3.
- [12] M. G. L. Roes, S. Member, J. L. Duarte, M. A. M. Hendrix, E. A. Lomonova, and S. Member, “Acoustic Energy Transfer : A Review,” in *IEEE Transactions On Industrial Electronics*, Jan, 2013, Vol. 60, No. 1, pp. 242–248.
- [13] A. Ekbote and D. S. Zinger, “Comparison of class e and half bridge inverters for use in electronic ballasts,” in *Industry Applications Conference, 2006*, Tampa, FL, 2006, vol. 5, pp. 2198–2201.
- [14] H. Koizumi, K. Kurokawa, and S. Mori, “Analysis of Class D Inverter With Irregular,” in *IEEE International Symposium on Circuits and Systems*, Vancouver, Canada, 2004 vol. 53, no. 3, pp. 677–687.
- [15] C. Brañas, F. J. Azcondo, and R. Casanueva, “A generalized study of multiphase parallel resonant inverters for high-power applications,” in *IEEE Transactions on Circuits and Systems*. 2008, *1 Regular Paper*, vol. 55, no. 7, pp. 2128–2138.
- [16] X. Wei and J. Liu, “Power sources and electrical recharging strategies for implantable medical devices,” in *Front. Energy Power Eng. China*, 2008, vol. 2, no. 1, pp. 1–13.
- [17] Marian K. Kazimierczuk, “Inverter,” in *Resonant Power Converters*, 2nd ed., New Jersey, John Wiley & Sons, 2010, ch 7, sec. 7.2-7.3, p. 193–217.